

# Effect of Surface Treatment on the Mechanical Properties of Glass Fiber/Vinylester Composites

Rohchoon Park,<sup>1</sup> Jyongsik Jang<sup>2</sup>

<sup>1</sup>R & D Center for Chemical Technology, Hyosung Corporation, 183, Hoge-Dong Dongan-Ku, Anyang-Si, Kyonggi-Do, South Korea

<sup>2</sup>School of Chemical Engineering, Seoul National University, San 56-1, Shinlimdong Kwanakgu, Seoul, South Korea

Received 26 February 2003; accepted 1 August 2003

**ABSTRACT:** To study the effect of surface treatment on the mechanical properties of glass fiber/vinylester composites, glass fiber was surface-treated with polybutadiene (PB),  $\gamma$ -methacryloxypropyltrimethoxysilane ( $\gamma$ -MPS), and  $\gamma$ -MPS-modified polybutadiene (PB/ $\gamma$ -MPS). The relationship between the interfacial strength and the impact strength of glass fiber/vinylester composites was also examined. PB/ $\gamma$ -MPS was synthesized as a new surface modifier. PB/ $\gamma$ -MPS-treated composites exhibited the optimum concentration at which the flexural strength and the interlaminar shear strength (ILSS) were maximized. This was related to the role of PB/ $\gamma$ -MPS in three interphase regions between the fiber and the matrix.

Considering the relationship between the interfacial strength and the impact strength of the composites, the propagation energy and total energy showed a different trend in three regions. In region A, the propagation energy and total energy increased with an increasing shear strength, indicating that the adequate interfacial strength was required for improving the impact strength of the composites. In region B, the propagation energy and total energy decreased with an increasing shear strength. Most of impact energy was absorbed through fiber pullout and delamination. In region C, the fiber breakage was the dominant failure mode of the composites. © 2004 Wiley Periodicals, Inc. *J Appl Polym Sci* 91: 3730–3736, 2004

## INTRODUCTION

Glass fiber-reinforced composites are attractive materials for the aerospace and automotive industries due to their high specific strength and stiffness, good formability, and excellent corrosion resistance. However, the advantages of these materials are significantly reduced because of their susceptibility to impact damage.<sup>1–5</sup>

Several approaches have been taken to improve the impact strength and damage tolerance of glass fiber-reinforced composites. The main research for toughened composites includes the control of the fiber–matrix interfacial adhesion,<sup>6</sup> matrix modification,<sup>7–9</sup> insertion of interlaminar interleaf layers,<sup>10</sup> and fiber hybridization.<sup>11–13</sup> Among the various methods, the control of the fiber–matrix interfacial adhesion appears to be very promising since it has a major effect on the impact strength of the composites. A variety of surface treatment and modification techniques has been developed to control the interfacial properties of glass fiber. These include the coating of glass fiber with a silane coupling agent,<sup>14,15</sup> polybutadiene, polysulfone, and silicon rubber.

Considering that the impact strength of glass fiber-reinforced composites is related to the interfacial

strength between the fiber and the matrix, it is very important to quantitatively define the relationship between the interfacial strength and the impact energy of the composites. The interfacial strength of the composites plays an important role in determining the failure modes and thus the impact energies of the composites. It is commonly thought that decreasing the interfacial strength can increase the amount of delamination, thus allowing the composite to absorb more impact energy. However, the systematic relationship between the interfacial strength and the impact strength of the composites has not been well understood.

In this study, we investigated the effect of the surface treatment of glass fiber on the mechanical properties of a glass fiber/vinylester composite using polybutadiene (PB),  $\gamma$ -methacryloxypropyltrimethoxysilane ( $\gamma$ -MPS), and  $\gamma$ -MPS-modified PB (PB/ $\gamma$ -MPS) as surface modifiers of glass fiber. We also explored the systematic relationship between the interfacial strength and the impact energy of glass fiber/vinylester composites.

## EXPERIMENTAL

### Materials

The glass fiber used in this study was a heat-treated plain fabric from Hankook Fiber Co. (Korea). The matrix resin was styrene-based XSR-10 vinylester resin supplied by the National Synthesis Co. (Korea). This resin is a carboxyl-terminated butadiene acrylo-

Correspondence to: R. Park.

nitrile (CTBN) rubber-modified vinylester resin with an improved impact property. The styrene contained in the vinylester resin was used as a crosslinking agent, and dibenzoyl peroxide (BPO) was used as the reaction initiator.

$\gamma$ -MPS, PB, and PB/ $\gamma$ -MPS were used as surface modifiers of the glass fiber.  $\gamma$ -MPS and PB were supplied by Petrach Systems and the Aldrich Chemical Co., respectively. PB has a number-average molecular weight of 5000 and contains 20% vinyl and 80% *cis* and *trans* units. PB/ $\gamma$ -MPS was synthesized using azobisisobutyronitrile (AIBN) as an initiator under a benzene solvent. The mol ratio of PB to  $\gamma$ -MPS was varied from 1 : 5 to 1 : 30, and the reaction was performed at 65°C for 18 h in a nitrogen atmosphere.

### Surface treatment of glass fiber

The PB solution was prepared using benzene as a solvent, and the glass fabric was impregnated into the PB solution. The PB-coated fabrics were dried at room temperature for 2 days in a hood. The amount of PB coating on the glass fiber was changed by the concentration of the PB solution. The PB concentration was varied from 0.1 to 0.7 wt %.

$\gamma$ -MPS and PB/ $\gamma$ -MPS were prehydrolyzed for 1 h in distilled water adjusted to pH 3.5 with acetic acid. The glass fabrics were impregnated in the prehydrolyzed solution for 10 min and dried for 2 days at room temperature in a hood. The concentration of  $\gamma$ -MPS and PB/ $\gamma$ -MPS was varied from 0.1 to 0.7 wt %.

### Composite manufacturing

The prepreg of glass fiber/vinylester composites was prepared using vinylester resin with 2 wt % dibenzoyl peroxide. Each fabric was well impregnated with a solution of this mixture in acetone by a hand roller. After drying for 2 days, 16-ply prepreps were laminated and then cured in a hot press for 20 min at 43°C and 50 min at 90°C under a pressure of 7 MPa. The thickness of the composites was fixed at about 2.0 mm.

### Fourier transformed infrared spectroscopy (FTIR)

A Bomem MB-100 FTIR with a deuterated triglycine sulfate (DTGS) detector was used to obtain FTIR spectra. The spectra of  $\gamma$ -MPS, PB, and PB/ $\gamma$ -MPS were obtained through a transmission technique by casting them on a KBr pellet. Dry nitrogen was purged to prevent the interference of atmospheric water and CO<sub>2</sub>. The resolution was fixed at 4 cm<sup>-1</sup> and a total of 32 scans were coadded.

### Flexural test

The flexural strength and modulus of the glass fiber/vinylester composites were measured using a three-

point bending test according to ASTM D 790. The length and width of the test specimens were 50 and 20 mm, respectively. The span length used was 32 mm, and the ratio of the span length to the sample thickness was adjusted to 16. The crosshead speed of the test was 1.3 mm/min. At least five samples were measured and the results were averaged.

### Interlaminar shear strength (ILSS)

The ILSS of the glass fiber/vinylester composites was determined using a universal testing machine (UTM) according to ASTM D 2344. Specimens were of the dimensions of 14 × 10 × 2 mm with a support span of 8 mm, and the crosshead speed was 2.0 mm/min.

### Impact test

The total impact energy absorbed during the penetration was measured using an RIT-4 high-rate impact tester from Rheometrics Co. The dimension of the test specimens was 10 × 10 cm. The impact velocity was fixed at 5.0 m/s. The probe diameter was 1.59 cm, and the load cell capability was 5000 lb.

### Scanning electron microscopy (SEM)

SEM was used to observe the fracture surface of glass fiber/vinylester composites. The instrument used in this experiment was a JEOL JSM-35 and all specimens were coated with a thin layer of gold to eliminate charging effects.

### Damage shape analysis

The deformation shape of the glass fiber/vinylester composites was analyzed using a manual camera after impact of the specimens. The back surface of the composites was observed to examine the relationship between the damaged shape and the absorbed impact energy.

## RESULTS AND DISCUSSION

PB/ $\gamma$ -MPS was synthesized as a new surface modifier of glass fiber. The analysis of PB/ $\gamma$ -MPS was carried out by an FTIR transmission technique. Figure 1 shows the FTIR transmission spectra of  $\gamma$ -MPS and PB/ $\gamma$ -MPS. Figure 1(a) is the spectrum of  $\gamma$ -MPS, showing the characteristic peaks at 1719 and 939 cm<sup>-1</sup>. The peak at 1719 cm<sup>-1</sup> is assigned to the carbonyl peak of the methacrylate group that is conjugated with the adjacent double bond. In addition, the band at 939 cm<sup>-1</sup> is associated with the wagging mode of the double bond within the methacrylate group. Figure 1(b) shows the change of the peaks of PB/ $\gamma$ -MPS compared with  $\gamma$ -MPS. The peak at 1728 cm<sup>-1</sup> origi-

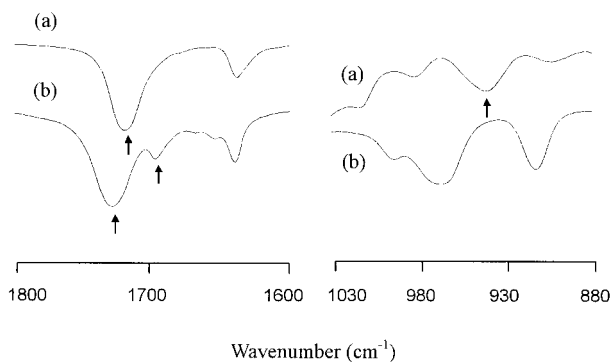


**Figure 1** FTIR transmission spectra of (a)  $\gamma$ -MPS and (b) PB/ $\gamma$ -MPS.

nates from the carbonyl group of PB/ $\gamma$ -MPS and is shifted to a higher wavenumber compared with  $\gamma$ -MPS. This is attributed to that the double bond adjacent to the carbonyl group disappears due to the reaction of PB with  $\gamma$ -MPS. The disappearance of conjugation enhances the electron density of the carbonyl group and leads to a higher frequency. In contrast with spectrum (a), the peak at  $939\text{ cm}^{-1}$  is not shown in spectrum (b). This indicates that the double bond of  $\gamma$ -MPS effectively reacts with that of PB. In addition, the peak at  $1696\text{ cm}^{-1}$  is due to the hydrogen bonding with water in air during the measurement.

FTIR absorbance spectra of PB and PB/ $\gamma$ -MPS are shown in Figure 2. Figure 2(a) is the spectrum of PB and exhibits the characteristic peaks at  $910$ ,  $960$ , and  $990\text{ cm}^{-1}$ . The peaks at  $910$  and  $990\text{ cm}^{-1}$  are associated with  $\text{CH}_2$  wagging and *trans*-CH wagging of the vinyl group, respectively. In addition, the peak at  $960\text{ cm}^{-1}$  is due to CH wagging of the *trans* group. Figure 2(b) is the spectrum of PB/ $\gamma$ -MPS and shows the same peak position as that of spectrum (a). However, the intensity of each peak is different in the two spectra. The peak intensity at  $910$  and  $990\text{ cm}^{-1}$  decreases

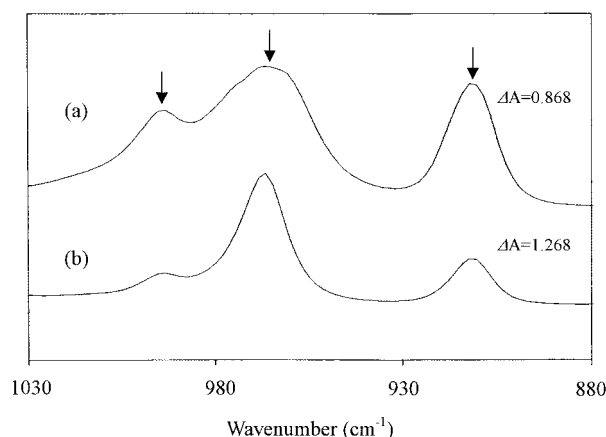


**Figure 2** FTIR absorbance spectra of (a) PB and (b) PB/ $\gamma$ -MPS.

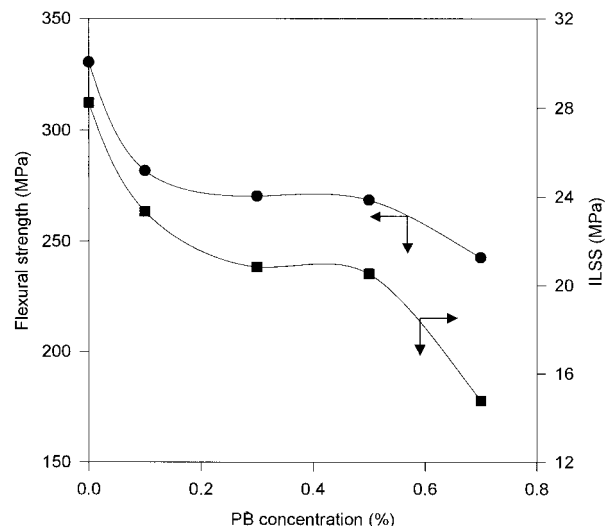


**Figure 3** Flexural strength and ILSS of glass fiber/vinylester composites according to PB concentration.

compared with spectrum (a). This suggests that the vinyl group of PB primarily reacts with the double bond of  $\gamma$ -MPS to form PB/ $\gamma$ -MPS.

The flexural strength and the ILSS of PB-treated glass fiber/vinylester composites as a function of the PB concentration are plotted in Figure 3. The flexural strength and the ILSS decrease continuously with an increase of the PB concentration. The PB treatment on the glass fiber gives rise to a decrease of about 25 and 45% in the flexural strength and the ILSS, respectively. The PB coated on the glass fiber surface results in a poor wetting and weak interface because PB has hydrophobic characteristics and cannot form a chemical bonding with the glass fiber. On loading, the long and flexible PB chains at the interphase region deform easily with a chain slippage and failure initiates in this region with a ductile behavior.

Figure 4 demonstrates the flexural strength and the ILSS of  $\gamma$ -MPS-treated glass fiber/vinylester composites. The values increase to a 0.3% concentration and then decrease smoothly after the maximum point. The  $\gamma$ -MPS contains hydroxyl groups that can react with the silanol groups on the glass fiber. The attachment on the glass fiber can thus be made through siloxane bonding by covalent bonds. In addition,  $\gamma$ -MPS contains the double bond at another end of chain that reacts with the vinylester resin during the curing process. Therefore, the  $\gamma$ -MPS acts as a bridge to bond the glass fiber to the vinylester resin with a chain of primary bonds. Above 0.3% concentration, however, physisorbed  $\gamma$ -MPS layers are formed on the chemisorbed layer by an excess amount. This layer acts as a lubricant or deformable layer, and the failure occurs in this region through the slippage of physisorbed  $\gamma$ -MPS chains.

Table I summarizes the flexural strength and ILSS of PB/ $\gamma$ -MPS-treated glass fiber/vinylester composites.

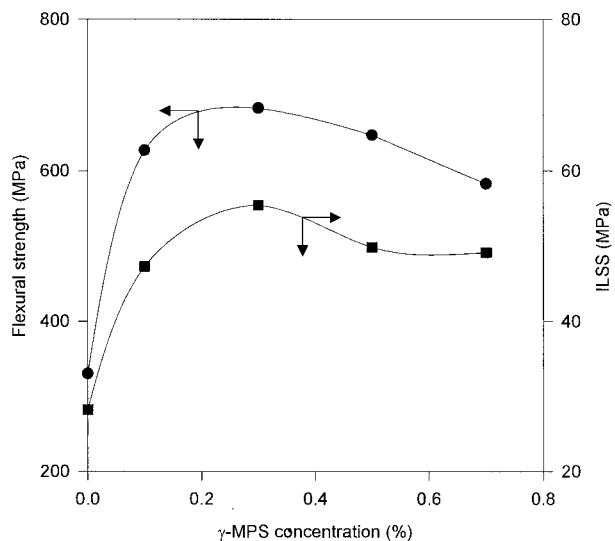


**Figure 4** Flexural strength and ILSS of glass fiber/vinylester composites according to  $\gamma$ -MPS concentration.

The mol ratio of PB to  $\gamma$ -MPS was varied from 1 : 5 to 1 : 30. The PB/ $\gamma$ -MPS with a mol ratio of 1 : 5 was denoted as PM5 and that of 1 : 30 was designated as PM30. All composites have the optimum concentration at which the flexural strength and ILSS are maximized. These phenomena can be explained by considering the interphase region between the fiber and the matrix. The role of PB/ $\gamma$ -MPS at the fiber–matrix interphase appears to be different in the three regions. First, the PB/ $\gamma$ -MPS in which the PB backbone chain is grafted by  $\gamma$ -MPS can form siloxane bonding with the silanol group of the glass fiber by  $\gamma$ -MPS components. This is a problem related to the region near the glass fiber surface (region 1). The second part is the bulk region of the fiber–matrix interphase (region 2). In this region, the entanglement between PB components ex-

ists because of their long and flexible characteristics. Although chemical bonding does not exist in this region, good bonding remains somewhat by chain entanglement. The last part is the region near the matrix resin (region 3). This region includes chemical bonding between double bonds of PB and the vinylester resin as well as the IPN through interdiffusion.

The glass fiber/vinylester composites exhibit different concentrations at which the flexural strength and ILSS are maximized depending on the role at each region. In this study, even at 0.1% concentration, several PB/ $\gamma$ -MPS layers can be formed on the glass fiber surface because its surface area is large enough. For a PM5-treated composite, the maximum flexural strength is observed at 0.1% concentration. PM5 can form chemical bonding with the glass fiber due to its  $\gamma$ -MPS component at region 1. As the concentration increases, a physisorbed layer is formed on the chemisorbed layer formed previously. Although a small degree of bonding is possible by entanglement between PB components, the interfacial strength at region 2 is weak compared with that of regions 1 and 3. Therefore, the failure of the composite occurs in this region with an increasing concentration. On the other hand, the PM9 and PM13 display the maximum flexural strength at higher concentrations. The PM9 and PM13 have more chance to react with the glass fiber due to an increase of the  $\gamma$ -MPS component at region 1. Moreover, region 2 includes siloxane bonding between the  $\gamma$ -MPS components of the PB/ $\gamma$ -MPS chain. Therefore, the increase of the  $\gamma$ -MPS component improves the interfacial strength at regions 1 and 2, and the applied load is well transferred to the glass fiber through these regions. In the case of PM17 and PM30, the maximum flexural strength is represented at a lower concentration. This is attributed to that the PB/ $\gamma$ -MPS chain does not have enough double bonds to

**TABLE I**  
Flexural Strength and ILSS of PB/ $\gamma$ -MPS-treated Glass Fiber/Vinylester Composites

Concentration (%)	PM5	PM9	PM13	PM17	PM30
Flexural strength (MPa)					
0.0	330.43	330.43	330.43	330.43	330.43
0.1	443.53	450.60	491.90	630.50	493.40
0.3	431.50	539.90	490.50	560.00	590.10
0.5	403.13	518.10	530.20	541.90	581.30
0.7	372.90	488.00	514.30	527.80	547.80
ILSS (MPa)					
0.0	28.23	28.23	28.23	28.23	28.23
0.1	33.64	32.90	37.95	47.84	38.83
0.3	31.49	33.09	34.48	41.49	42.84
0.5	30.21	32.62	33.46	40.97	44.30
0.7	25.75	27.74	28.60	38.24	42.75



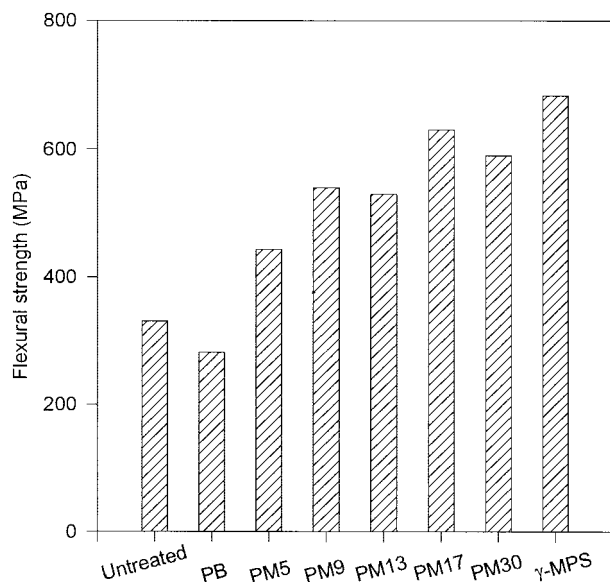


**Figure 5** Maximum flexural strength of glass fiber/vinylester composites treated with various PB/ $\gamma$ -MPS.

react with the vinylester matrix. Therefore, region 3 is a locus of failure due to the scarcity of chemical bonding and IPN.

The maximum flexural strength of the glass fiber/vinylester composites treated with various PB/ $\gamma$ -MPSs is shown in Figure 5. The PM17-treated composite exhibits the highest value of all the PM-treated composites. This is related to the structure of PB/ $\gamma$ -MPS according to the mol ratio. The reaction of PB with  $\gamma$ -MPS occurs primarily at the double bond of the vinyl group due to steric hindrance. The PB used in this experiment has about 19 double bonds of the vinyl group. In the mol ratio of 1 : 17, half of the vinyl group reacts with  $\gamma$ -MPS because  $\gamma$ -MPS exists mainly in a dimer or oligomer form and the rest of the vinyl group reacts with the double bond of the vinylester matrix during the curing process. This results in the optimal conformation of PB/ $\gamma$ -MPS in reaction with the glass fiber and the vinylester resin.

The impact strength of the fiber-reinforced composite is related to the interfacial strength between the fiber and the matrix. Therefore, it is very important to quantitatively define the relationship between the interfacial strength and the impact energy of the composites. Figure 6 exhibits the correlation between the ILSS and the impact energy of the glass fiber/vinylester composites. It can be seen that the initiation energy increases more or less with an increasing shear strength. For a composite with good interfacial strength, the load can be transferred more adequately from the matrix to the fiber, and the transverse strength of the composite increases. During the impact, therefore, the stress required to cause cracking between the transverse fibers becomes greater. On the

other hand, the propagation energy and the total energy exhibit a different trend at the three regions. In region A, the propagation energy and the total energy increase with an increasing shear strength. At a very low shear strength, the impact load leads to the easy separation of the fiber-matrix interface and the impact energy cannot be effectively absorbed. This is due to the absence of the load-bearing capability of the composite. Therefore, adequate interfacial strength is required for improving the impact property of the composites. In region B, the propagation energy and the total energy decrease with an increasing shear strength. The fiber pullout and delamination appear to be the dominant failure mode in this case. The weak interfacial strength can increase the amount of the fiber pullout and delamination, thus allowing the composite to absorb more impact energy with a large damage area. On the other hand, the strong bonding at the fiber-matrix interface tends to restrain fiber pullout and delamination, which results in a decrease of the propagation energy and total energy with a small damage area. Above a critical value of shear strength, the propagation energy and total energy increase with an increasing the shear strength (region C). The fiber breakage is the dominant failure mode of the composites. In this case, the degree of delamination is considerably less and most of impact energy is dissipated through the breakage of fibers during the initial load drop.

Figure 7 shows the fracture surface of the composites treated with various surface modifiers after impact. The fracture surface of the representative composite contained in region A [Fig. 7(a)] shows the clean

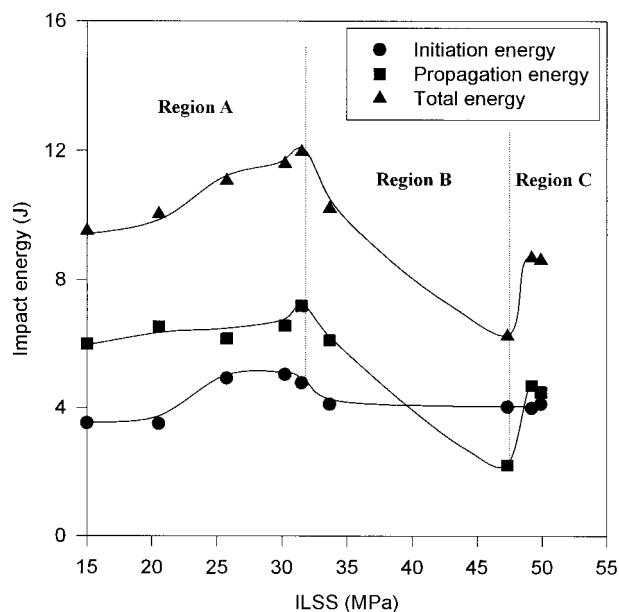


**Figure 6** Relationship between ILSS and impact energy of glass fiber/vinylester composites.

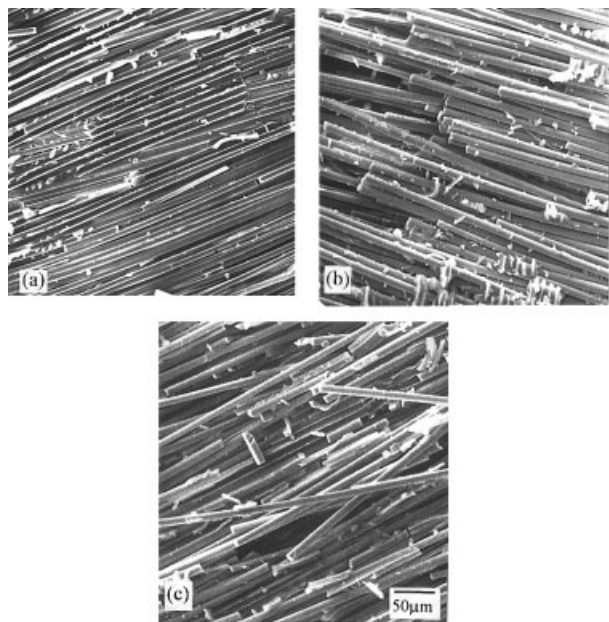


**Figure 7** Fracture surface of glass fiber/vinylester composites treated with various surface modifiers after impact: (a) region A; (b) region B; (c) region C.

fiber surface with little matrix damage, indicating that the fiber–matrix debonding occurs along the longitudinal direction of fiber due to the low interfacial strength. For the composite included in region B [Fig. 7(b)], it is clear that the fiber pullout is the major mechanism to absorb the impact energy. As the crack propagates, it pulls out the broken fiber from the matrix, giving rise to a continuation of the post-debonding frictional work. Much impact energy is dissipated into the longitudinal direction of the fiber through this process. The fracture surface of the composite included in region C [Fig. 7(c)] exhibits much fiber breakage. The crack propagates through the fiber breakage rather than through the interface between the fiber and the matrix. This indicates that the impact failure mechanism of the composite changes to a brittle manner because of the high interfacial strength.

Photographs showing the fracture surfaces of various composites after impact are represented in Figure 8. All the photographs show the back surfaces of the composites. The composite in region A [Fig. 8(a)] and the composite in region B [Fig. 8(b)] show a cross-shaped crack, indicating that the impact energy is dissipated into the multidirection with an enlarged damage area. This is attributed to the extensive deformation of the composite through fiber–matrix debonding and fiber pullout. On the other hand, the composite in region C appears to experience a brittle response to the impact load [Fig. 8(c)]. The high stress generated near the impact point results in easy penetration and perforation with a small damage zone.

**CONCLUSIONS**

The effect of the surface treatment of the glass fiber on the mechanical properties of glass fiber/vinylester composites was investigated. PB/ $\gamma$ -MPS was synthesized as a new surface modifier. For PB-treated composites, the PB treatment on the glass fiber decreased the flexural strength and ILSS because PB has hydrophobic characteristics and cannot form chemical bonding with the glass fiber. For  $\gamma$ -MPS-treated composites,  $\gamma$ -MPS acted as a bridge to bond the glass fiber to the vinylester resin. PB/ $\gamma$ -MPS-treated composites showed the optimum concentration at which the flexural strength and ILSS were maximized. This was related to the role of PB/ $\gamma$ -MPS in three interphase regions between the fiber and the matrix. The PM17-treated composite exhibited the highest interfacial strength of all the PM-treated composites. This was attributed to that PM17 had an optimal conformation in the reaction with the glass fiber and vinylester resin. The relationship between the interfacial strength and the impact strength of the glass fiber/vinylester composites was also examined. The propagation energy and total energy exhibited different trends at the three regions. In region A, the propagation energy and total energy increased with an increasing shear strength, indicating that adequate interfacial strength was required for improving the impact strength of the composites. In region B, the propagation energy and the total energy decreased with an increasing shear strength. Most of the impact energy was absorbed through fiber pullout and delamination. In region C,

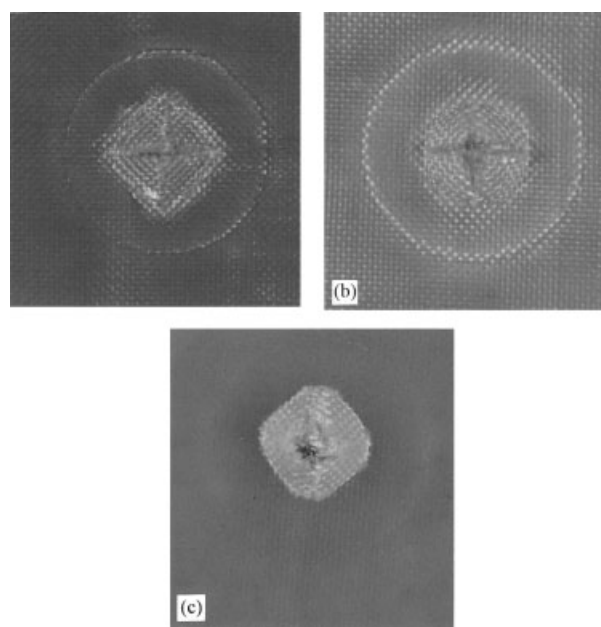


**Figure 8** Photographs showing the fracture surfaces of glass fiber/vinylester composites after impact: (a) region A; (b) region B; (c) region C.

the fiber breakage was the dominant failure mode of the composites and most of impact energy was dissipated through the breakage of the fibers.

### References

1. Hancox, N. L. *Fiber Composite Hybrid Materials*; Applied Science: London, 1981.
2. Mallick, P. K.; Newman, S. *Composite Materials Technology*; Hanser: New York, 1990.
3. Benzeggagh, M. L.; Benmedakhene. *Comp Sci Technol* 1995, 55, 1.
4. Updegraff, I. H. *Handbook of Composites*; Van Nostrand Reinhold: New York, 1990.
5. Kocsis, J. K. *Comp Sci Technol* 1993, 30, 273.
6. Yeung, P.; Broutman, L. *J Polym Eng Sci* 1978, 18, 62.
7. Jang, B. Z.; Panus, J.; Wang, C. Z. *Proc 34th Int SAMPE Symp* 1989.
8. Collings, T. A. *Composites* 1991, 22, 369.
9. Chandra, D. S.; Avadhani, G. S.; Kishore. *Mater Sci Eng A* 1991, 136, 179.
10. Krieger, R. B. *Adv Mater Technol* 1987, 32, 279.
11. McColl, I. R.; Morley, J. G. *J Mater Sci* 1977, 12, 1165.
12. Jang, B. Z.; Chen, L. C.; Wang, C. Z.; Lin, H. T.; Zee, R. H. *Comp Sci Technol* 1989, 34, 305.
13. Harris, B.; Bunsell, A. R. *Composites* 1975, 6, 197.
14. Plueddeman, E. P. *Silane Coupling Agent*; Plenum: New York, 1989.
15. Suzuki, Y.; Saitoh, J. *Proc 34th Int SAMPE Symp* 1989, 2031.